

## Many-Body Renormalization of Semiconductor Quantum Wire Excitons: Absorption, Gain, Binding, and Unbinding

S. Das Sarma and D. W. Wang

*Department of Physics, University of Maryland,  
College Park, Maryland 20742-4111*

(Received 4 May 1999)

We consider theoretically the formation and stability of quasi-one-dimensional many-body excitons in GaAs quantum wire structures under external photoexcitation conditions by solving the dynamically screened Bethe-Salpeter equation for realistic Coulomb interaction. In agreement with several recent experimental findings the calculated excitonic peak shows weak carrier-density dependence up to (and even above) the Mott transition density,  $n_c \sim 3 \times 10^5 \text{ cm}^{-1}$ . Above  $n_c$  we find considerable optical gain demonstrating compellingly the possibility of a one-dimensional quantum wire laser operation.

PACS numbers: 78.55.-m, 71.35.Cc, 73.20.Dx, 78.66.Fd

An exciton, the bound Coulombic (“hydrogenic”) state between an electron in the conduction band and a hole in the valence band, is an extensively studied central concept in semiconductor physics. Recent interest has focused on low dimensional excitons in artificially structured semiconductor quantum well or wire systems where carrier confinement may substantially enhance the excitonic binding energy leading to novel optical phenomena. In this Letter we consider the formation, stability, and optical properties of one-dimensional (1D) excitons in semiconductor quantum wires, a problem which has attracted a great deal of recent experimental [1–3] and theoretical [4–6] attention. Our motivation has been a number of recent puzzling experimental observations [1,2], which find the photoluminescence emitted from an initially photoexcited semiconductor quantum wire plasma to be peaked essentially at a *constant* energy independent of the magnitude of the photoexcitation intensity. This is surprising because one expects a strongly density-dependent “redshift” in the peak due to the exchange-correlation induced band gap renormalization (BGR) (i.e., a shrinkage of the fundamental band gap due to electron and hole self-energy corrections), which should vary strongly as a function of the photoexcited electron-hole density [7–9]. This striking lack of any dependence of the observed photoluminescence peak energy on the photoexcitation density has led to the suggestion [1,2] that the observed quantum wire photoluminescence may be arising entirely from an excitonic [as opposed to an electron-hole plasma (EHP)] recombination mechanism. The effective excitonic energy is a constant (as a function of carrier density) in 1D quantum wires due to a near exact cancellation between the redshift arising from the self-energy correction induced BGR and the blueshift arising from screening induced excitonic binding weakening. In this Letter, focusing on the photoexcited quasiequilibrium regime, we provide a quantitative theory for this problem by solving for the first time the full many-body dynamical Bethe-Salpeter equation for 1D excitons. We include both self-energy renormalization and

vertex correction (arising from the Coulomb interaction) on an equal footing under high photoexcitation conditions. (Note that since the many-body Bethe-Salpeter equation is far more complex than the single-exciton Wannier equation, several commonly used excitonic concepts, such as exciton radius, binding energy, or Mott transition, become imprecise and ambiguous in our full theory. For simplicity, however, we use these terminologies to qualitatively interpret our results.) We find that in agreement with experimental observations, our calculated effective excitonic energy (indicating the luminescence peak frequency) remains essentially a constant (with an energy shift of less than 0.5 meV) as a function of 1D carrier density  $n$  for  $n < n_c \sim 3 \times 10^5 \text{ cm}^{-1}$  with the system making a Mott transition from an insulating exciton gas of bound electron-hole pairs ( $n < n_c$ ) to an EHP ( $n > n_c$ ) at  $n = n_c$ . For  $n > n_c$  we find strong optical gain in the calculated absorption spectra.

For our results to be presented here, the many-body exciton is given by the so-called Bethe-Salpeter equation [10] for the two-particle Green’s function which is shown diagrammatically in Fig. 1. The many-body diagrams shown in Fig. 1 correspond to a rather complex set of two-component (electrons and holes) coupled nonlinear integral equations which must be solved self-consistently with the bare interaction being the Coulomb interaction. These equations are notoriously difficult to solve without making drastic approximations, and, in fact, have never before been solved in the literature *in any dimensions*. We use the parabolic band effective mass approximation considering the highest valence and the lowest conduction band only. In carrying out the full many-body dynamical calculation for the Bethe-Salpeter equation we are forced to make some approximations. Our most sophisticated approximation uses the fully frequency dependent dynamically screened electron-hole Coulomb interaction in the single plasmon-pole approximation, which has been shown to be an excellent approximation [11] to the full random phase approximation [RPA, see Fig. 1(c)] for 1D quantum

wire dynamical screening. For the self-energy correction we use the single-loop  $GW$  diagram shown in Fig. 1(b). Ward Identities then fix the vertex correction, entering Fig. 1(a), to be the appropriate ladder integral equation.

After considerable algebra [10] the reduced form of the Bethe-Salpeter equation for the electron-hole two-particle Green's function,  $G_{eh}$ , (spin,  $s$ , has been included in the summation over momentum,  $k$ ) becomes

$$G_{eh}(k, k', \omega) = G_{eh}^0(k, k', \omega) \left[ \delta_{kk'} - \sum_{k''} V_{\text{eff}}(k'', k', \omega) G_{eh}(k'', k', \omega) \delta_{ss''} \right], \quad (1)$$

where  $G_{eh}^0$  and the effective dynamical electron-hole interaction,  $V_{\text{eff}}$ , are expressed as

$$G_{eh}^0(k, k', \omega) = \frac{1 - f_e(e_{e,k}) - f_h(e_{h,-k})}{\omega + i\delta - \varepsilon_{e,k} - \varepsilon_{h,-k} - \Delta_{eh}(k, \omega)}, \quad (2)$$

and

$$V_{\text{eff}}(k, k', \omega) = \left( \frac{1}{\beta} \right)^2 \sum_{z, z'} \left[ \frac{G_e(k, \Omega - z) + G_h(-k, z)}{1 - f_e(e_{e,k}) - f_h(e_{h,-k})} V(k - k', z - z') \frac{G_e(k', \Omega - z') + G_h(-k', z')}{1 - f_e(e_{e,k'}) - f_h(e_{h,-k'})} \right]. \quad (3)$$

Here  $\Omega \equiv \omega - \mu_e - \mu_h + i\delta$  and  $f_i$ ,  $G_i$ ,  $\varepsilon_i$ ,  $e_i$ , and  $\mu_i$  are the Fermi function, one-particle Green's function, noninteracting kinetic energy, interacting kinetic energy (including self-energy), and chemical potential of electron ( $i = e$ ) or hole ( $i = h$ ), respectively. The dynamically screened Coulomb potential,  $V(k, \omega)$ , is approximated as  $V(k, \omega) = V(k) \left( 1 + \frac{\omega_0^2}{\omega^2 - \omega_k^2 + i\delta} \right)$ , where  $\omega_k$  is the effective plasma frequency of the system in RPA and the strength  $\omega_0$  is determined by satisfying the  $f$ -sum rule [11]. The 1D bare Coulomb interaction,  $V(k)$ , is calculated by averaging the real 3D Coulomb interaction through the wave functions of electrons and holes over the transverse 2D section of a real 70 Å GaAlAs-GaAs  $T$ -junction quantum wire system [1]. (We emphasize the importance of using the real Coulomb interaction in the calculation. Various model interactions, such as the delta function one used in Ref. [6], are not particularly meaningful from either a

theoretical perspective or in understanding experimental data.) This expression of  $V(k, \omega)$  enables us to perform the frequency summations in  $V_{\text{eff}}$  analytically, making the numerical calculations in Eq. (1) tractable. The effective BGR,  $\Delta_{eh}$ , is given by

$$\Delta_{eh}(k, \omega) = \sum_{k'} \{ [1 - f_e(e_{e,k'}) - f_h(e_{h,-k'})] \times V_{\text{eff}}(k, k', \omega) - V(k - k') \} \delta_{ss'}. \quad (4)$$

In our calculation, both real and imaginary parts of self-energy are included in the Green's function,  $G_i$ , and therefore the broadening and lifetime effects in our results are intrinsically theoretically calculated quantities and *not* artificially introduced phenomenological fitting parameters.

Before solving the full Bethe-Salpeter equation, it is instructive to study the excitonic and EHP effects *separately* by treating the influence of the plasma on the excitonic states as a perturbation [10]. Using an effective Hamiltonian derived from the Bethe-Salpeter equation, we can obtain the exciton energy by minimizing the energy expectation value variationally through a  $1s$  excitonic trial wave function (see Fig. 2). The effective Hamiltonian treats EHP as a perturbative effect and is written as  $H_{pp'}(\omega_n) = H_{pp'}^0 + H'_{pp'}(\omega_n)$ , where  $H^0$  is for the single electron-hole pair and the perturbation  $H'$  is

$$H'_{pp'}(\omega_n) = \Delta_{eh}(p, \omega_n) \delta_{pp'} + V(p - p') - [1 - f_e(e_{e,k}) - f_h(e_{h,-k})] V_{\text{eff}}(k, k', \omega_n), \quad (5)$$

for the  $n$ th eigenstate of energy  $\omega_n$ . Note that the variational calculation, which follows the procedure described in [10], is quantitatively valid only when the exciton-plasma hybridization is not particularly strong. For the purpose of comparison we also show as an inset in Fig. 2 the purely *one-electron* static screening result where

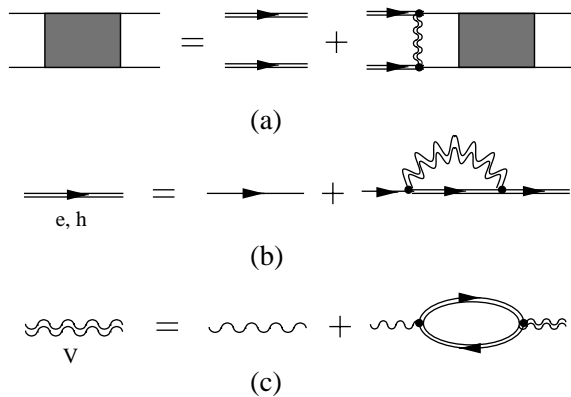


FIG. 1. Many-body Feynman diagrams used in the theory with the single (double) solid line representing the bare (dressed) electron ( $e$ ) or hole ( $h$ ) Green's function, the single (double) wavy line representing the bare (dressed) Coulomb interaction: (a) the excitonic Bethe-Salpeter equation; (b) the single-loop self-energy (in the so-called  $GW$  approximation) defining the dressed Green's function; (c) the RPA dressing of the Coulomb interaction (treated in the plasmon-pole approximation in our calculation). The interaction includes  $e$ - $e$ ,  $h$ - $h$ , and  $e$ - $h$  terms.

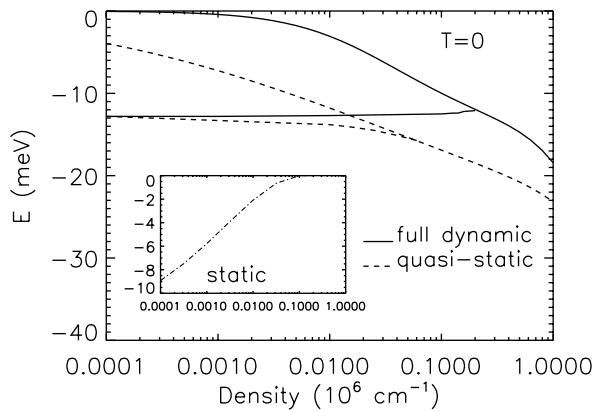


FIG. 2. Shows variationally calculated exciton energy and BGR of the EHP as a function of photoexcitation carrier density. The heavy lines are the exciton energy and the light lines are the BGR correction obtained from the self-energy diagram [Fig. 1(b) with 1(c)] neglecting the excitonic binding effect. We compare the results of the full dynamical screening (solid lines) and quasistatic (dashed lines) approximations as described in the text. The Mott transition occurs at the density ( $n_c$ ) where the heavy and the light lines cross indicating the exciton merging with the band continuum. The inset shows the exciton binding energy in the statically screened interaction neglecting BGR effects.

the electron-hole interaction is modeled by the density-dependent statically screened interaction, and all many-body effects (e.g., BGR) are ignored. The quasistatic approximation, which is formally described in Ref. [10], shown as dashed lines in Fig. 2, involves making the screened exchange plus Coulomb hole approximation in the self-energy diagrams neglecting the correlation hole effect. (Note that in the pure Hartree-Fock approximation one neglects screening altogether.) Comparing the three (static, quasistatic, and dynamic) approximations one could see the importance of dynamical effects in the highly photoexcited quantum system. The large blueshift of static screening (inset) could not be canceled by the many-body self-energy effects within the same static screening approximation, and therefore totally disagree with the experimental findings. Inclusion of dynamical many-body effects, shown in the results in the main part of Fig. 2, qualitatively modifies the situation: (1) for density between  $10^4$  and  $10^5$   $\text{cm}^{-3}$  the exciton energy has a few meV redshift in the quasistatic approximation and almost no shift (less than 0.5 meV blueshift) in the dynamical screening approximation; (2) the Mott transition density for the quasistatic approximation is about  $10^5$   $\text{cm}^{-3}$ , while it is about  $3 \times 10^5$   $\text{cm}^{-3}$  for the dynamical theory; (3) below  $n_c$  our variational solution corresponds to a quasi-1D  $1s$  excitonic wave function with a radius of about 100–500 Å [12], and this description is approximately valid until  $n_c$ , above which the calculated excitonic wave function is completely delocalized (with a very large radius) and the EHP becomes the dominant state of the system.

In Fig. 3, we show our calculated absorption and gain spectra by solving the full Bethe-Salpeter equation in the

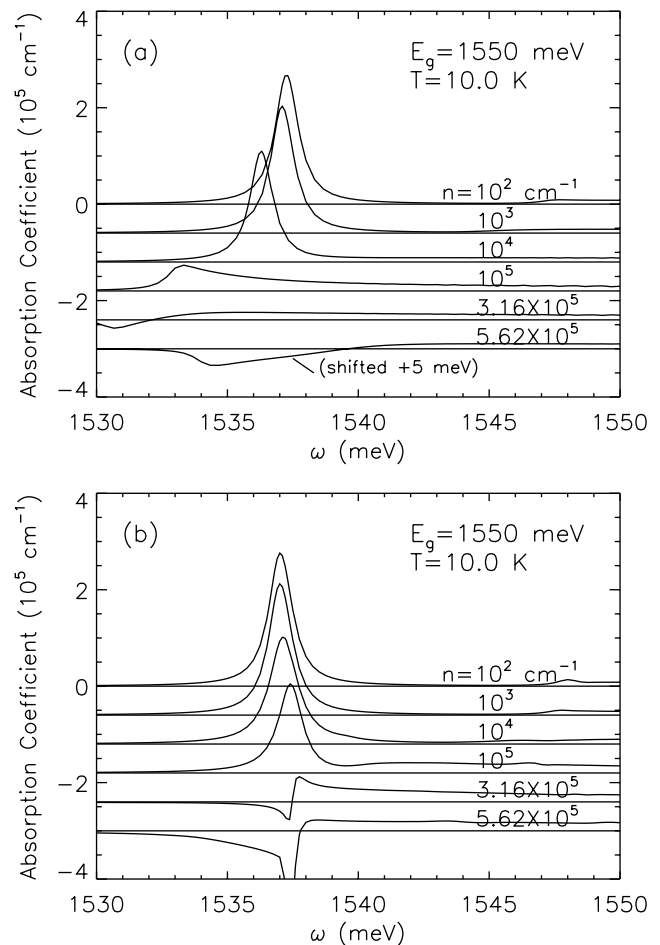


FIG. 3. Calculated absorption and gain spectra for various photoexcitation densities by solving the full Bethe-Salpeter equation: (a) the quasistatic approximation, and (b) the dynamical approximation. Negative absorption indicates gain.

quasistatic and the dynamical screening approximations. The integral equation for the two-particle Green's function, Eq. (1), is solved by the matrix inversion method. The dynamical screening approximation, together with the logarithmic singularity of the 1D Coulomb interaction, produces a multisingular kernel with multiple momentum-dependent singularities which have never been solved in the literature before. The usual singularity-removal method is ineffective here. This fact forces us to use a rather large matrix (about  $1500 \times 1500$  in a Gaussian quadrature) in the matrix inversion method in order to get good overall accuracy. Some important features of the optical spectra shown in Fig. 3 are (1) there are generally two absorption peaks in the low density ( $n < 10^4$   $\text{cm}^{-3}$ ) spectra, one is the exciton peak at 1537 meV and the other one is the band edge peak at, for example, 1547.5 meV for  $n = 10^2$   $\text{cm}^{-3}$  in Fig. 3(b). The exciton peak has much larger oscillator strength than the band edge peak. (2) At low densities ( $n < 10^4$   $\text{cm}^{-3}$ ) the exciton peak does not shift much ( $\sim 1537$  meV) with increasing carrier density (in either approximation), indicating the effective constancy of the exciton energy; (3) at higher densities,

however, the quasistatic approximation produces a redshift in the excitonic peak by a few meV, consistent with the result shown in Fig. 2 which is obtained variationally. However, also consistent with the results shown in Fig. 2, the excitonic peak of the full dynamical screening approximation is almost a constant (with only a 0.5 meV blueshift) up to  $n_c$ . (4) Below the Mott density, the excitonic oscillator strength decreases rapidly as the carrier density increases in the quasistatic approximation; however, it remains almost a constant with increasing carrier density in the dynamical screening approximation, indicating the interesting prospect of excitonic lasing in 1D quantum wires. (5) In the dynamical screening approximation, considerable excitonic gain is achieved for  $n > n_c$  without any observable energy shift in the spectrum. We find [12] that at very high densities ( $n > 10^6 \text{ cm}^{-3}$ ) the excitonic features in the absorption spectra are smeared out by the EHP continuum, and the BGR induced redshift is observed. In Fig. 4, we show the absorption spectra at  $n = 0.8 \times 10^5 \text{ cm}^{-3}$  for various temperatures. The absorption peak has a clear redshift in energy as the temperature increases, and the oscillator strength is also weakened, together with the broadened absorption peak, in the high temperature spectra. This result is consistent with very recent experimental results [13].

We note that our dynamical screening Bethe-Salpeter equation results are in excellent qualitative and quantitative agreement with the recent experimental findings [1,2]. In particular, the effective constancy of the exciton peak as a function of the photoexcited carrier density as well as the possibility of excitonic absorption and lasing well into the high density regime (even for  $n > n_c \sim 3 \times 10^5 \text{ cm}^{-3}$ ) turns out to be characteristic features of the full dynamical theory (but *not* of the static and the quasistatic approximation). A full dynamical self-consistent theory as developed in this Letter is thus needed for an understanding of the recent experimental observations. We also note that in the recent literature the Mott density for 1D GaAs quantum wire systems has often been quoted as  $n_c \sim 8 \times 10^5 \text{ cm}^{-3}$  which is substantially higher than our dynamical theory result,  $n_c \sim 3 \times 10^5 \text{ cm}^{-3}$ . The higher value of  $n_c$  follows from the simplistic estimates based on Hartree-Fock type energetic calculations, which neglect dynamical screening effects completely and consequently strongly (and incorrectly) overestimate the stability of the bound excitonic state. The actual  $n_c$  has never been experimentally measured since there is no simple or direct method of measuring the density of a photoexcited  $e$ - $h$  plasma.

In summary, our main accomplishments reported in this Letter are the following: (1) The *first* fully dynamical theory of a photoexcited electron-hole system in semiconductors which treats self-energy, vertex corrections, and dynamical screening in a self-consistent scheme based on the  $GW$  self-energy and ladder-bubble vertex-polarization diagrams within a realistic Coulomb interaction-based Bethe-Salpeter theory; (2) a reasonable qualitative and quantitative agreement with the recent experimental

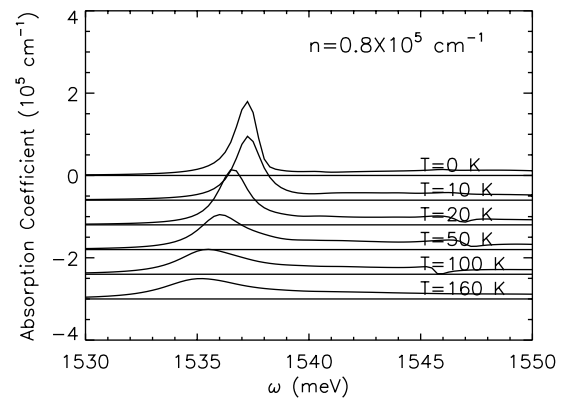


FIG. 4. The absorption and gain spectra for various temperatures at the photoexcitation density  $n = 0.8 \times 10^5 \text{ cm}^{-3}$ , calculated by the full dynamical Bethe-Salpeter equation.

observations of an effectively (photoexcitation density-independent) constant exciton peak, which in our dynamical theory arises from an approximate cancellation of self-energy and vertex corrections in the Bethe-Salpeter equation; (3) an effective 1D quantum wire Mott transition density of  $n_c \sim 3 \times 10^5 \text{ cm}^{-3}$  which is below earlier estimates based on less sophisticated approximations; (4) the concrete theoretical demonstration of the possibility of excitonic gain and lasing in 1D quantum wire structures in the density range of  $n > 3 \times 10^5 \text{ cm}^{-3}$  where considerable optical gain is achieved in our calculated absorption spectra.

This work has been supported by the US-ONR and the US-ARO.

- 
- [1] W. Wegscheider *et al.*, Phys. Rev. Lett. **71**, 4071 (1993).
  - [2] R. Ambigapathy *et al.*, Phys. Rev. Lett. **78**, 3579 (1997).
  - [3] R. Rinaldi *et al.*, Phys. Rev. B **59**, 2230 (1999).
  - [4] S. Glutsch *et al.*, Phys. Rev. B **56**, 4108 (1997); D. Brinkmann and G. Fishman, *ibid.* **56**, 15 211 (1997); S.N. Walck *et al.*, *ibid.* **56**, 9235 (1997); M. Grundmann and D. Bimberg, *ibid.* **55**, 4054 (1997).
  - [5] T. Ogawa and T. Takagahara, Phys. Rev. B **44**, 8138 (1991); S. Glutsch *et al.*, *ibid.* **51**, 16 885 (1995); F. Rossi and E. Molinari, Phys. Rev. Lett. **76**, 3642 (1996); F. Rossi *et al.*, *ibid.* **78**, 3527 (1997).
  - [6] F. Tassone and C. Piermarocchi, Phys. Rev. Lett. **82**, 843 (1999).
  - [7] B. Y. K. Hu and S. Das Sarma, Phys. Rev. B **48**, 5469 (1993); E. H. Hwang and S. Das Sarma, *ibid.* **58**, R1738 (1998).
  - [8] S. Benner and H. Haug, Europhys. Lett. **16**, 579 (1991); B. Tanatar, J. Phys. Condens. Matter **8**, 5997 (1996); C. Greus *et al.*, Europhys. Lett. **34**, 213 (1996).
  - [9] R. Cingolani *et al.*, Phys. Rev. B **48**, 14 331 (1993); K. H. Wang *et al.*, Phys. Rev. B **53**, R10 505 (1996).
  - [10] H. Haug and S. Schmitt-Rink, Prog. Quantum. Electron. **9**, 3 (1984).
  - [11] S. Das Sarma, E. H. Hwang, and L. Zheng, Phys. Rev. B **54**, 8057 (1996).
  - [12] D. W. Wang and S. Das Sarma (unpublished).
  - [13] J. Rubio *et al.* (to be published).